**Supplementary material**

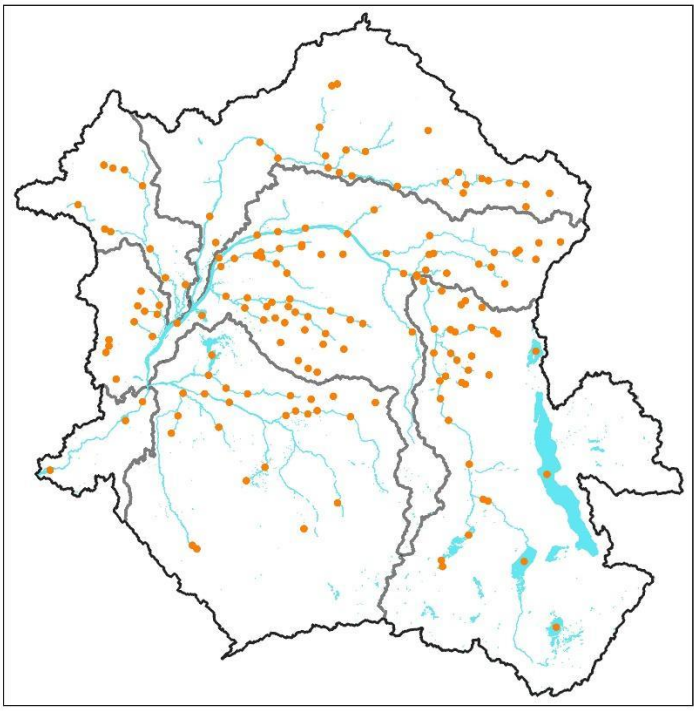

Figure S1. Locations of long-term radar altimetry VSs from the pooling of ERS-2, ENV, and SRL satellite missions within the CRB.

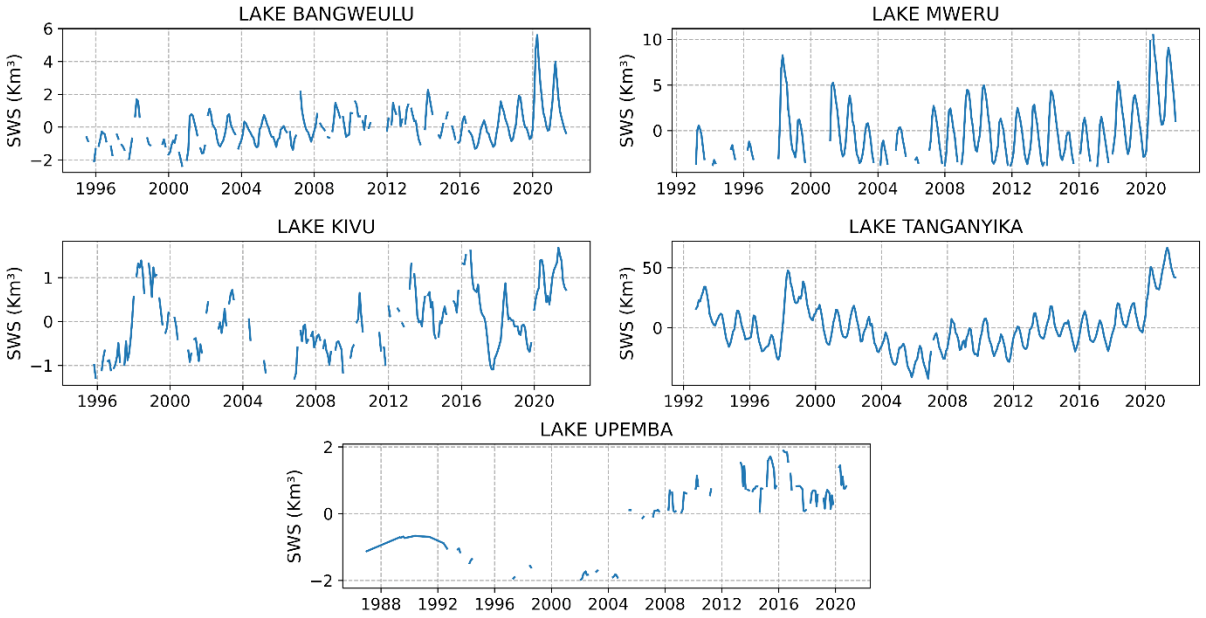


Figure S2. Water volume anomaly time series of five large lakes included in the sum of SWS anomaly variations. The reference point for calculating the volume change is the first water area from Pekel dataset ((https://global-surface-water.appspot.com/download) and height measurement from HydroSat database (http://hydrosat.gis. uni-stuttgart.de/).

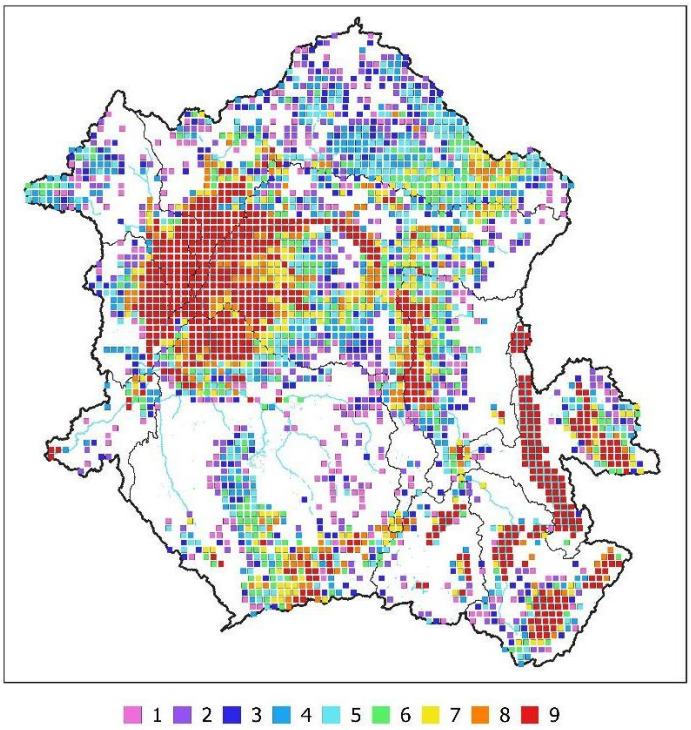


Figure S3. Map of agreement showing how many times a pixel of hypsometric curve (from FABDEM) is represented in connection with different STD used to derive the hypsometric curve. For instance, numerical number 1 (magenta) means, from different attempts of STD ranging from 0.3 to 1.1 m, one value of STD allows to generate the hypsometric curve. 2 (violet) means, among different attempts of STD, two value of STD enables to generate the hypsometric curve, and so on. 9 (red) shows pixel of hypsometric curve derived with all th e range (0.3-1.1 m) of STD.

As shown in Fig. S3, the calculation of the hypsometric curve for a specific STD generates several pixels over the basin. For example, using STD of 0.7, the generated pixels of hypsometric curve are estimated to be 2856 over the Congo basin. Not all generated pixels are relevant in the estimation of SWS anomaly. Among 2856 pixels, we considered only pixels that correspond to GIEMS-2 pixels with almost one month of inundation data (pixels classified as wetland). The number of GIEMS-2 pixels with almost one month of inundation data is 767. With this number, only 563 pixels out of 767 represented the SWS anomaly variation over the basin. The remain pixels gave a storage of zero due to the following reasons (1) pixels located generally in the highland of eastern and southern part show higher variation of STD due to the topographic conditions of the region. This lead to do not manage applying the correction of the hypsometric curve with the derived elevation amplitude largely above the defined range. Thus, the associated pixels are set aside. (2) pixels located on lakes do not show variations in elevation. So, the derived hypsometric curve is flat, thus the elevation amplitude is zero and leading to a storage of zero. (3) pixels inundated only once over the period 1992-2015 with a value of less than 5 $Km^2$ lead to a storage of zero as well due the computation process.

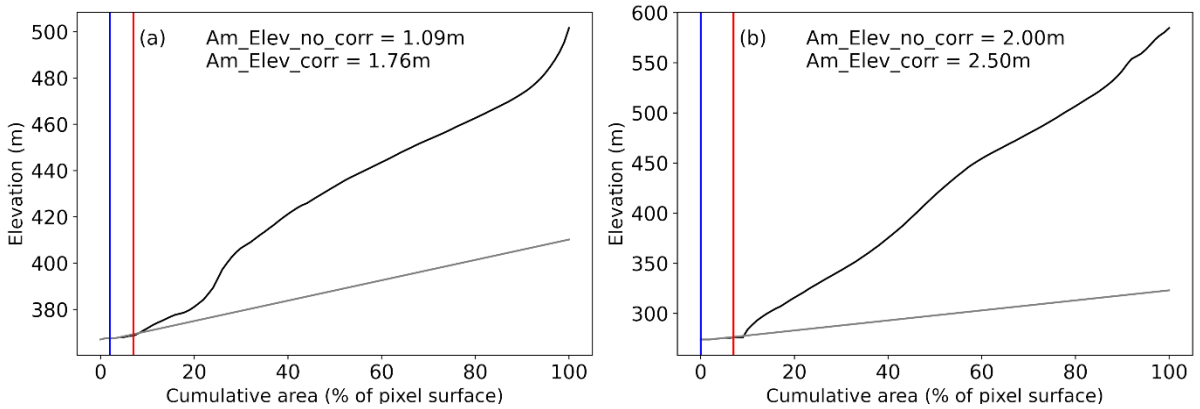


Figure S4. Uncommon error during correction of hypsometric curve (from FABDEM). (a) and (b) show slight increasing of the elevation amplitude after applying the correction described at step (2) of section 4.2. Am_Elev_no_corr (from none-corrected curve) and Am_Elev_corr (from corrected curve) are the elevation amplitude derived from the minimum (blue line) and maximum (red line) average coverage of SWE observed by GIEMS-2 over 1992-2015.

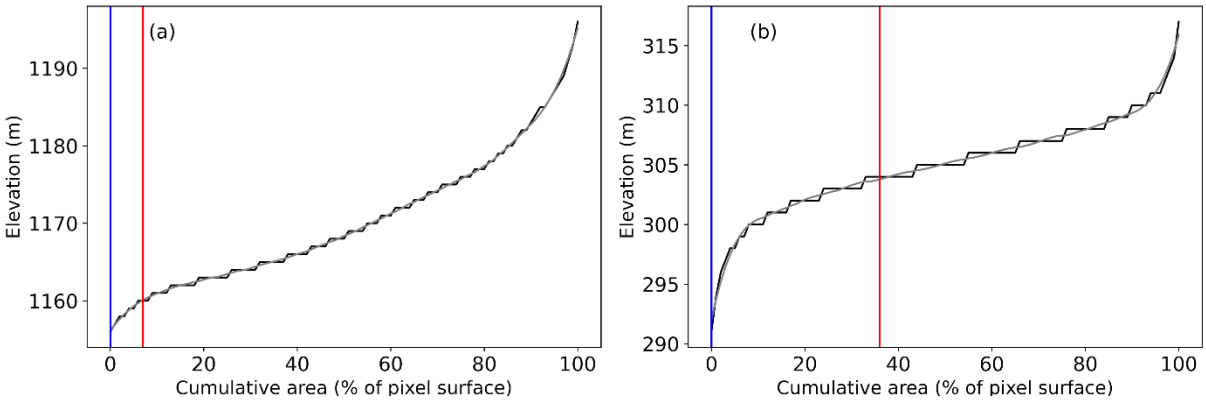


Figure S5. Smoothing of the hypsometric curve from ALOS (a) and ASTER (b) GDEMs showing roughness using Savitzky-Golay filter. The blue (red) line is the minimum (maximum) average coverage of SWE observed by GIEMS-2 over 1992-2015. The gray curve is the derived-hypsometric curve from considered GDEMs and the black curve is the corrected hypsometric curve.

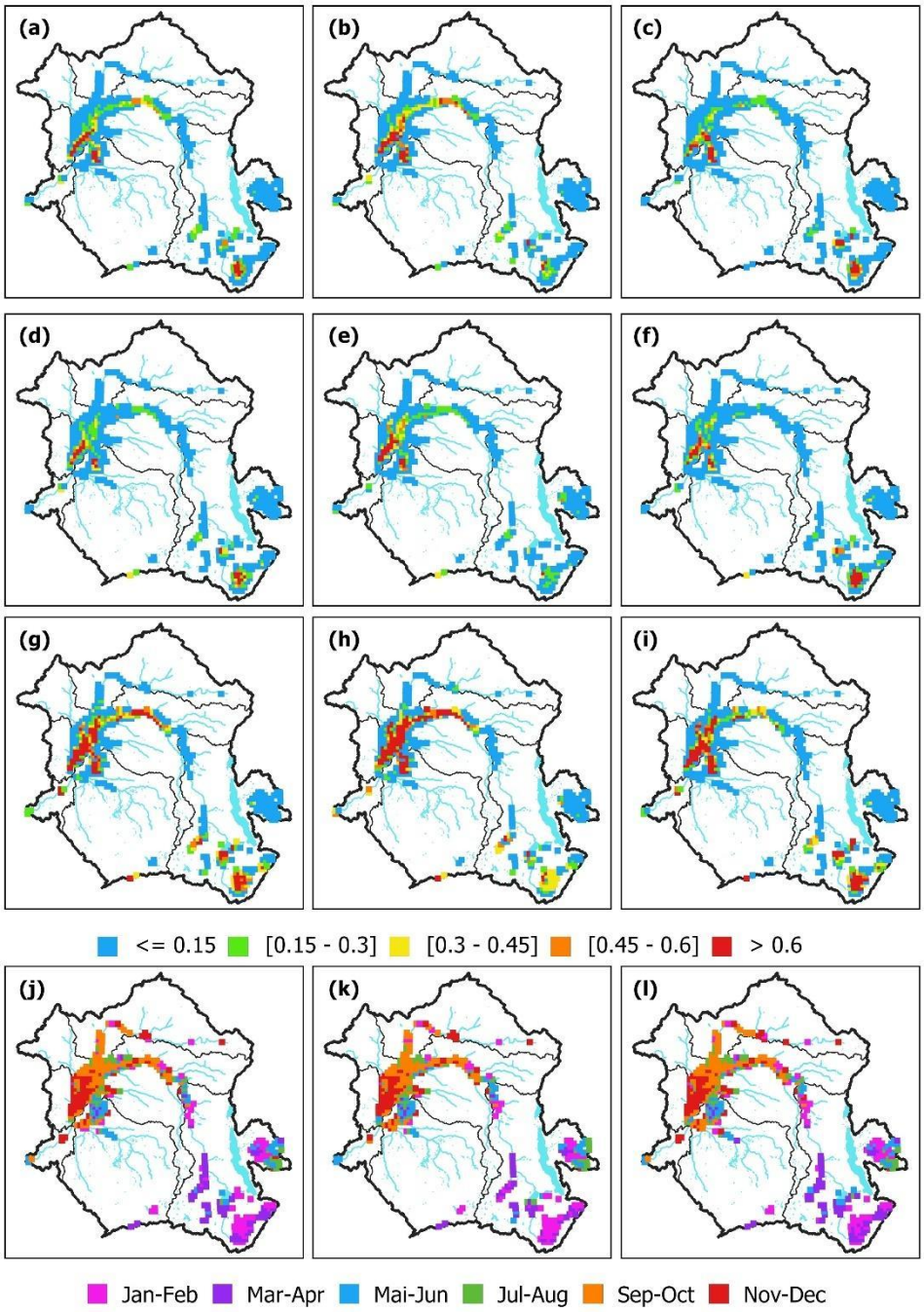


Figure S6. Spatial characterization of the CRB's SWS anomaly variations. Mean annual [(a), (b), (c)] in $km^3$, Standard Deviation [(d), (e), (f)] in $km^3$, Mean annual maximum [(g), (h), (i)] in $km^3$, and Mean month of the maximum [(j), (k), (l)] in month averaged over 1992– 2015 from ALOS (left column), ASTER (centre column), and MERIT (right column) GDEMs calculating using hypsometric approach for each 773 $km^2$ pixel.